PHYSICAL REVIEW B **89**, 245443 (2014)

Spin Hall and Edelstein effects in metallic films: From two to three dimensions

J. Borge,[1] C. Gorini,[2] G. Vignale,[3] and R. Raimondi[1]
[1]*Dipartimento di Matematica e Fisica, Università Roma Tre, Via della Vasca Navale 84, Rome, 1-00146 Italy*
[2]*Service de Physique de l'État Condensé, CNRS URA 2464, CEA Saclay, F-91191 Gif-sur-Yvette, France*
[3]*Department of Physics and Astronomy, University of Missouri, Columbia, Missouri 65211, USA*
(Received 18 March 2014; revised manuscript received 9 June 2014; published 26 June 2014)

A normal metallic film sandwiched between two insulators may have strong spin-orbit coupling near the metal-insulator interfaces, even if spin-orbit coupling is negligible in the bulk of the film. In this paper, we study two technologically important and deeply interconnected effects that arise from interfacial spin-orbit coupling in metallic films. The first is the spin Hall effect, whereby a charge current in the plane of the film is partially converted into an orthogonal spin current in the same plane. The second is the Edelstein effect, in which a charge current produces an in-plane, transverse spin polarization. At variance with strictly two-dimensional Rashba systems, we find that the spin Hall conductivity has a finite value even if spin-orbit interaction with impurities is neglected and "vertex corrections" are properly taken into account. Even more remarkably, such a finite value becomes "universal" in a certain configuration. This is a direct consequence of the spatial dependence of spin-orbit coupling on the third dimension, perpendicular to the plane of the film. The nonvanishing spin Hall conductivity has a profound influence on the Edelstein effect, which we show to consist of two terms, the first with the standard form valid in a strictly two-dimensional Rashba system, and a second arising from the presence of the third dimension. Whereas the standard term is proportional to the momentum relaxation time, the new one scales with the spin relaxation time. Our results, although derived in a specific model, should be valid rather generally, whenever a spatially dependent Rashba spin-orbit coupling is present and the electron motion is not strictly two dimensional.

DOI: 10.1103/PhysRevB.89.245443 PACS number(s): 75.70.Tj, 72.25.−b, 75.76.+j

I. INTRODUCTION

Spin-orbit coupling gives rise to several interesting transport phenomena arising from the induced correlation between charge and spin degrees of freedom. In particular, it allows one to manipulate spins without using magnetic electrodes, having as such become one of the most studied topics within the field of spintronics [1–14]. Among the many interesting effects that arise from spin-orbit coupling, two stand out for their potential technological importance: the spin Hall effect [15] and the Edelstein effect [16,17]. The spin Hall effect consists in the appearance of a z-polarized spin current flowing in the y direction produced by an electric field in the x direction [18–22]. The generation of a perpendicular electric field by an injected spin current, i.e., the inverse spin Hall effect, has been observed in numerous settings and presently provides the basis for one of the most effective methods to detect spin currents [23–25]. The Edelstein effect [16,17] consists instead in the appearance of a y-spin polarization in response to an applied electric field in the x direction. It has been proposed as a promising way of achieving all-electrical control of magnetic properties in electronic circuits [18,19,26–31]. The two effects are deeply connected [32–34], as we will see momentarily.

There are, in principle, several possible mechanisms for the spin Hall effect, and it is useful to divide them in two classes. We call them either extrinsic or intrinsic, depending on whether their origin is the spin-orbit interaction with impurities or with the regular lattice structure. In this work, we will focus exclusively on intrinsic effects. This means that the impurities (while, of course, needed to give the system a finite electrical conductivity) do not couple to the electron spin.

Bychkov and Rashba devised an extremely simple and yet powerful model [35] describing the intrinsic spin-orbit coupling of the electrons in a two-dimensional electron gas (2DEG) in a quantum well in the presence of an electric field perpendicular to the plane in which the electrons move. In spite of its apparent simplicity, this analytically solvable model has several subtle features, which arise from the interplay of spin-orbit coupling and impurity scattering. The best-known feature is the vanishing of the spin Hall conductivity (SHC) for a uniform and constant in-plane electric field [36–38]. This would leave spin-orbit coupling with impurities (not included in the original Bychkov-Rashba model) as the only plausible mechanism for the experimentally observed spin Hall effect in semiconductor-based 2DEGs [18,19].[1]

However it has been recently pointed out that the vanishing of the SHC need not occur in systems which are not strictly two dimensional, as explicitly shown in a model schematically describing the interface of the two insulating oxides $LaAlO_3$ and $SrTiO_3$ (LAO/STO) [40]. Even more recently [41], it has been suggested that a large SHC could be realized in a thin metal (Cu) film that is sandwiched between two different insulators, such as oxides or even the vacuum.[2] Such a system is shown schematically in Fig. 1. The inversion symmetry breaking across the interfaces produces interfacial Rashba-type spin-orbit couplings, thus allowing metals without substantial intrinsic bulk spin-orbit to host a nonvanishing SHC. The spin-orbit coupling asymmetry or,

[1]An alternative source of intrinsic spin Hall effect is random fluctuations of the electric field perpendicular to the 2DEG (see Dugaev *et al.* [39]).

[2]A very large spin Hall angle of extrinsic origin has been observed [51] in thin films of Cu doped with bismuth impurities. In Ref. [41], however, the Bi impurities are absent.

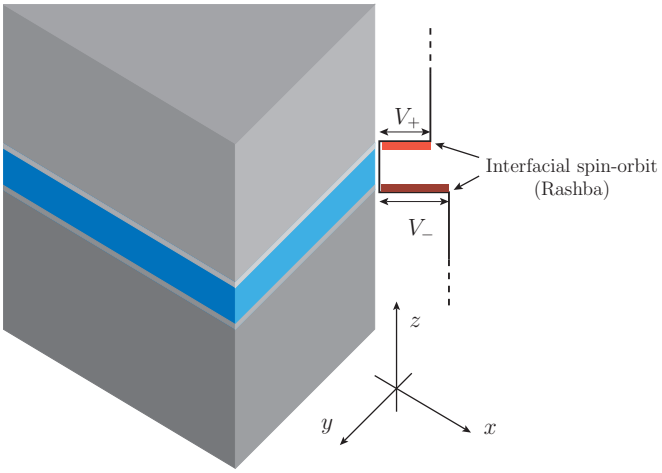

FIG. 1. (Color online) Schematic representation of a thin metal film sandwiched between insulators with asymmetric interfacial spin-orbit couplings. V_+ and V_- are the heights of the two interfacial potential barriers. These potentials generate interfacial spin-orbit interactions of the Rashba type, whose strength is controlled by the effective Compton wavelengths λ_+ and λ_- respectively.

more generally, the fact that the spin-orbit interaction is not homogeneous across the thickness of the film, is the core issue in this approach. In this paper, we will study the influence of the interfacial spin-orbit couplings on the Edelstein and spin Hall effects in this class of heterostructures.

Before proceeding to a detailed study of the model depicted in Fig. 1, it is useful to recall the connection [32–34] that exists between the spin Hall and Edelstein effects in the Bychkov-Rashba model, described by the Hamiltonian

$$H = \frac{p^2}{2m} + \alpha(\sigma_x p_y - \sigma_y p_x), \tag{1}$$

where m is the effective electron mass and α is the Bychkov-Rashba spin-orbit coupling constant given by $\alpha = \lambda^2 e E_z/\hbar$, with λ the materials' effective Compton wavelength, E_z the electric field perpendicular to the electron layer, and e the absolute value of the electron charge. It is convenient to describe spin-orbit coupling in terms of a non-Abelian gauge field $\boldsymbol{\mathcal{A}} = \mathcal{A}^a \sigma^a/2$, with $\mathcal{A}^x_y = 2m\alpha$ and $\mathcal{A}^y_x = -2m\alpha$ [43–45]. If not otherwise specified, superscripts indicate spin components, while subscripts stand for spatial components. The first consequence of resorting to this language is the appearance of an SU(2) magnetic field $\mathcal{B}^z_z = -(2m\alpha)^2$, which arises from the noncommuting components of the Bychkov-Rashba vector potential. Such a spin-magnetic field couples the charge current driven by an electric field, say along x, to the z-polarized spin current flowing along y. This is very much similar to the standard Hall effect, where two *charge* currents flowing perpendicular to each other are coupled by a magnetic field. The drift component of the spin current can thus be described by a Hall-type term

$$\left[J^z_y\right]_{\text{drift}} = \sigma^{\text{SHE}}_{\text{drift}} E_x. \tag{2}$$

It is, however, important to appreciate that this is not yet the full spin Hall current, i.e., $\sigma^{\text{SHE}}_{\text{drift}}$ is not the full SHC. In the diffusive regime, $\sigma^{\text{SHE}}_{\text{drift}}$ is given by the classic formula $\sigma^{\text{SHE}}_{\text{drift}} = (\omega_c \tau)\sigma_D/e$, where $\omega_c = \mathcal{B}/m\hbar$ is the "cyclotron frequency" associated with the SU(2) magnetic field, τ is the elastic momentum scattering time, and σ_D is the Drude conductivity. For a more general formula, see Eq. (6).

In addition to the drift current, there is also a "diffusion current" due to spin precession around the Bychkov-Rashba effective spin-orbit field. Within the SU(2) formalism, this current arises from the replacement of the ordinary derivative with the SU(2) covariant derivative in the expression for the diffusion current. The SU(2) covariant derivative, due to the gauge field, is

$$\nabla_j \mathcal{O} = \partial_j \mathcal{O} + i[\mathcal{A}_j, \mathcal{O}], \tag{3}$$

with $\mathcal{O}$ a given quantity being acted upon. The normal derivative ∂_j along a given axis j is shifted by the commutator with the gauge field component along that same axis. As a result of the replacement $\partial \to \nabla$ diffusionlike terms, normally proportional to spin density gradients, arise even in uniform conditions and the diffusion contribution to the spin current turns out to be

$$\left[J^z_y\right]_{\text{diff}} = \frac{2m\alpha}{\hbar} D s^y, \tag{4}$$

where $D = v_F^2 \tau/2$ is the diffusion coefficient, v_F being the Fermi velocity. In the diffusive regime, the full spin current J^z_y can thus be expressed in the suggestive form

$$J^z_y = \frac{D}{L_{\text{so}}} s^y + \sigma^{\text{SHE}}_{\text{drift}} E_x, \tag{5}$$

where $L_{\text{so}} = \hbar(2m\alpha)^{-1}$ plays the role of an "orientational spin diffusion length" related to the different Fermi momenta in the two spin-orbit split bands. For a detailed justification of Eq. (5), we refer the reader to Refs. [44,46]. The factor in front of the spin density in the first term of Eq. (5) can also be written in terms of the Dyakonov-Perel spin relaxation time, i.e., the "orientational spin diffusion time" given by $\tau_s = L^2_{\text{so}}/D$. In terms of τ and τ_s one has

$$\sigma^{\text{SHE}}_{\text{drift}} = \frac{e}{8\pi\hbar}\frac{2\tau}{\tau_s}, \tag{6}$$

which is indeed equivalent to the classical surmise given after Eq. (2). If we introduce the total SHC and the Edelstein conductivity (EC) defined by

$$J^z_y = \sigma^{\text{SHE}} E_x, \quad s^y = \sigma^{\text{EE}} E_x \tag{7}$$

we may rewrite Eq. (5) as

$$\sigma^{\text{EE}} = \frac{\tau_s}{L_{so}}\left(\sigma^{\text{SHE}} - \sigma^{\text{SHE}}_{\text{drift}}\right). \tag{8}$$

In the standard Bychkov-Rashba model, a general constraint from the equation of motion dictates that under steady and uniform conditions $J^z_y = 0$. Therefore, the EC reads as

$$\sigma^{\text{EE}} = -\frac{\tau_s}{L_{so}}\sigma^{\text{SHE}}_{\text{drift}} = -e\frac{m}{2\pi\hbar^2}\alpha\tau = -eN_0\alpha\tau, \tag{9}$$

which is easily obtained by using the expressions given above and the single-particle density of states in two dimensions $N_0 = m/2\pi\hbar^2$. The remarkable thing is that this expression remains unchanged for arbitrary ratios between the spin splitting energy and the disorder broadening of the levels. However, in a more general situation with a nonzero SHC,

the EC would consist of the two terms appearing in Eq. (8). The latter equation is the "deep connection" mentioned earlier between the Edelstein and the spin Hall effect. The second term on the right-hand side is the "regular" contribution to the EC, the only surviving one in the Bychkov-Rashba model where the full SHC vanishes. The first term is "anomalous" in the sense that it does not appear in the standard Bychkov-Rashba model, but it does appear in more general models such as the one we discuss in this paper. Notice that the "regular" term is proportional to τ [see Eq. (6)], while the "anomalous" term is proportional to the Dyakonov-Perel relaxation time τ_s, which, in the diffusive regime, is *inversely* proportional to the momentum relaxation time.

At variance with the Bychkov-Rashba model, the model we choose for our system is not strictly two dimensional, and we take into account several states of quantized motion (subbands) in the direction perpendicular to the interface (z). A crucial feature of this model is the occurrence of two different spin-orbit couplings at the two interfaces. The difference arises because (i) the interfacial potential barriers V_+ and V_- are generally different, and (ii) the effective Compton wavelengths λ_+ and λ_-, characterizing the spin-orbit coupling strength at the two interfaces, are different.

Our central results for the generic asymmetric model are

$$\sigma^{\mathrm{SHE}} = -\sum_{n=1}^{n_c} \frac{e}{4\pi\hbar} \frac{\Delta E^{(3)}_{nk_{Fn}}}{\Delta E_{nk_{Fn}}} \tag{10}$$

and

$$\sigma^{\mathrm{EE}} = \sum_{n=1}^{n_c} \frac{eN_0}{k_{Fn}\hbar} \left[\Delta E_{nk_{Fn}}\tau + \Delta E^{(3)}_{nk_{Fn}} \tau^{(n)}_{\mathrm{DP}}\right], \tag{11}$$

the sums running over the n_c filled z subbands of the thin film. To each subband there corresponds a Fermi wave vector (without spin orbit) k_{Fn}, an intraband spin-orbit energy splitting with a linear- and a cubic-in-k part

$$\Delta E_{nk_{Fn}} = (2E_0 n^2/d)\left[k_{Fn}(\lambda_+^2 - \lambda_-^2) + \frac{2mk_{Fn}^3}{\hbar^2}(\lambda_+^6 V_+ - \lambda_-^6 V_-)\right] \tag{12}$$

$$\equiv \Delta E^{(1)}_{nk_{Fn}} + \Delta E^{(3)}_{nk_{Fn}} \tag{13}$$

and a Dyakonov-Perel spin relaxation time

$$\frac{\tau^{(n)}_{\mathrm{DP}}}{\tau} = 2\left[\frac{1 + \left(2\tau\Delta E_{nk_{Fn}}/\hbar\right)^2}{\left(2\tau\Delta E_{nk_{Fn}}/\hbar\right)^2}\right]. \tag{14}$$

In the above formulas, d is the film thickness and $E_0 = \hbar^2\pi^2/2md^2$. It is important to keep in mind that these formulas have been derived under the following assumptions:

(1) The spin-orbit interaction produces only a small correction to the energy levels: in particular, the spin splittings ΔE_{nk} in the various subbands are small in comparison with the energy separation between the subbands, which we denote by ΔE_{IB}. By considering the first term in Eq. (12) and assuming the interband spacing scaling as E_0, this assumption requires the effective Compton wavelength to be smaller than the geometrical average between the film thickness and the Fermi wavelength $\lambda_\pm < \sqrt{d\lambda_{F_n}}$ with $\lambda_{F_n} = 2\pi/k_{F_n}$. The second term in Eq. (12) is also assumed small with respect to the first as required for the validity of the expansion, implying the condition $2mk_{Fn}^2 V_\pm \lambda_\pm^4/\hbar^2 < 1$. Hence, in summary, one requires the conditions

$$\frac{\lambda_\pm^2}{d\lambda_{F_n}} < 1, \quad \frac{V}{E_0} < \frac{d^2\lambda_{F_n}^2}{\lambda_\pm^4}. \tag{15}$$

As a rough estimate with $d \sim 10^{-9}$ m, $\lambda_\pm \sim 10^{-10}$ m, $\lambda_{F_n} \sim 10^{-9}$ m, we have $\lambda_\pm^2/(d\lambda_{F_n}) \sim 10^{-2}$, which makes the assumption (15) reasonable.

(2) In addition, the spacing between subbands must be large compared to the broadening caused by disorder, meaning that interband transitions caused by impurity scattering are rare. Mathematically, this condition is expressed by the inequality

$$\frac{\hbar}{\tau} < \Delta E_{\mathrm{IB}}, \tag{16}$$

where τ is the typical electron-impurity scattering time. This condition implies, in particular, that the metallic film can not be too large, otherwise the intersubband spacing, scaling as $E_0 \sim 1/d^2$, would become smaller than $\hbar/\tau$. A corollary to this is that the number of occupied subbands must remain small, for example, one has $n_c = 4$ in a typical 1-nm-wide Al film [47]. Roughly, one expects $\Delta E_{\mathrm{IB}}\tau/\hbar \sim 10$.

Two particularly interesting regimes are apparent. First, a "quasisymmetric" configuration, defined by equal spin-orbit strengths $\lambda_+ = \lambda_- \equiv \lambda$, but different barrier heights $V_+ \neq V_-$. In this case, $\Delta E^{(1)}_{nk} = 0$ (due to Ehrenfest's theorem[3]) and a most striking result is obtained: the SHC has a maximal value of $-\frac{e}{4\pi\hbar}$ (independent of λ!) times the number of occupied bands

$$\sigma^{\mathrm{SHE}} = -\sum_{n=1}^{n_c} \frac{e}{4\pi\hbar}. \tag{17}$$

At the same time, the "anomalous" EC is at its largest. A second very interesting configuration is a strongly asymmetric insulator-metal-vacuum junction $\lambda_- \ll \lambda_+ \equiv \lambda$, $V_- \gg V_+ \equiv V$. In this case, the SHC becomes directly proportional to the barrier height V on the side on which the spin-orbit interaction is stronger:

$$\sigma^{\mathrm{SHE}} = -\sum_{n=1}^{n_c} \frac{e}{4\pi\hbar^3} 2mk_{Fn}^2 V\lambda^4. \tag{18}$$

Notice that, in view of condition (15), the SHC can not be made arbitrarily large simply by engineering a large V.

The paper is organized as follows. In Sec. II, we introduce and discuss the model. In Secs. III and IV, we calculate the SHC and the EC, respectively. Both sections are technically

[3]This is because the splitting of the energy levels to first order in k is shown by perturbation theory to be proportional to the expectation value of $V'(z)$, i.e., the force, in the ground state in the absence of spin-orbit coupling. By Ehrenfest's theorem this is the expectation value of the time derivative of the z component of the momentum, and therefore must vanish [52].

heavy and can be skipped at a first reading, leading straight to Sec. V where the physical consequences of our results are discussed and special regimes are analyzed. Section VI presents our summary and conclusions.

II. THE MODEL AND ITS SOLUTION

Following Ref. [41], we model the normal metallic thin film via the following Hamiltonian:

$$H = \frac{p^2}{2m} + \frac{p_z^2}{2m} + V_C(z) + H_R + U(\mathbf{r}), \tag{19}$$

where the first term represents the kinetic energy associated to the unconstrained motion in the xy plane and $\mathbf{p} = (p_x, p_y)$ is the two-dimensional momentum operator. The second term is the kinetic energy of the motion in the perpendicular direction, with p_z the momentum operator in the z direction (we ignore the possibility of different effective masses in plane and out of plane). The finite thickness d of the metallic film is taken into account by a confining potential

$$V_C = V_+\theta(z - z_+) + V_-\theta(z_- - z), \tag{20}$$

where $V_\pm$ is the height of the potential barrier at $z_\pm = \pm d/2$ and $\theta(z)$ is the Heaviside function. The third term in Eq. (19) describes the Rashba interfacial spin-orbit interaction in the xy plane located at $z_\pm = \pm d/2$:

$$H_R = \frac{\lambda_-^2 V_-\delta(z - z_-) - \lambda_+^2 V_+\delta(z - z_+)}{\hbar}(p_y\sigma_x - p_x\sigma_y), \tag{21}$$

where $\lambda_\pm$ are the effective Compton wavelengths for the two interfaces, $\sigma_x, \sigma_y, \sigma_z$ are the Pauli matrices. The last term in Eq. (19) represents the scattering from impurities affecting the motion in the x-y plane and $\mathbf{r} = (x, y)$ is the coordinate operator. The impurity potential is taken in a standard way as a white-noise disorder with variance $\langle U(\mathbf{r})U(\mathbf{r}')\rangle = (2\pi N_0\tau)^{-1}\delta(\mathbf{r} - \mathbf{r}')$, where N_0 is the two-dimensional density of states previously introduced. We will assume throughout that the Fermi energy E_{Fn} in each subband is much larger than the level broadening $\hbar/\tau$ and use the self-consistent Born approximation.

The eigenfunctions of the Hamiltonian (19) have the form

$$\psi_{n\mathbf{k}s}(\mathbf{r}, z) = \frac{e^{i\mathbf{k}\cdot\mathbf{r}}}{\sqrt{\mathcal{A}}}\frac{1}{\sqrt{2}}\begin{pmatrix} 1 \\ ise^{i\theta_\mathbf{k}} \end{pmatrix} f_{n\mathbf{k}s}(z), \tag{22}$$

where $\mathcal{A}$ is the area of the interface, $\mathbf{k} = (k_x, k_y)$ is the in-plane wave vector, $\mathbf{r}$ is the position in the interfacial plane, and z is the coordinate perpendicular to the plane. $\theta_\mathbf{k}$ is the angle between $\mathbf{k}$ and the x axis. These states are classified by a *subband index* $n = 1, 2, \ldots$, which plays the role of a principal quantum number, an in-plane wave vector $\mathbf{k}$, and a *helicity index* $s = +1$ or -1 which determines the form of the spin-dependent part of the wave function.

By inserting the wave function (22) into the Schrödinger equation for the Hamiltonian (19), we find the following equation for the functions $f_{n\mathbf{k}s}(z)$ describing the motion along the z axis:

$$-\frac{\hbar^2}{2m}f''_{n\mathbf{k}s}(z) + \{V_C(z) - ks[\lambda_-^2 V_-\delta(z + d/2) - \lambda_+^2 V_+\delta(z - d/2)]\}f_{n\mathbf{k}s}(z) = \epsilon_{n\mathbf{k}s} f_{n\mathbf{k}s}(z), \tag{23}$$

where the full energy eigenvalues are

$$E_{n\mathbf{k}s} = \frac{\hbar^2 k^2}{2m} + \epsilon_{n\mathbf{k}s}. \tag{24}$$

By taking into account the continuity of the wave function $f_{n\mathbf{k}s}(z)$ at $z = \pm d/2$ and the discontinuities of its derivatives we obtain for the eigenvalue $\epsilon_{n\mathbf{k}s}$ the following transcendental equation:

$$\arctan\left(\frac{\sqrt{\epsilon}}{\sqrt{\left(\frac{d^2}{d_-^2} - \epsilon\right)} - \frac{d}{d_-}\alpha_- sk}\right) + \arctan\left(\frac{\sqrt{\epsilon}}{\sqrt{\left(\frac{d^2}{d_+^2} - \epsilon\right)} + \frac{d}{d_+}\alpha_+ sk}\right) + \sqrt{\epsilon} = n\pi, \tag{25}$$

where the energy ϵ is measured in units of $E_0/(\pi^2) = \hbar^2/(2md^2)$ set by the thickness of the film. In the absence of spin-orbit coupling ($\lambda_\pm = 0$) and for infinite heights of the potential ($V_\pm \to \infty$), the solution reduces to the well-known energy levels $\epsilon_{n\mathbf{k}s} = E_0 n^2$.

In the general case with both $\lambda_\pm$ and $V_\pm$ finite, we use perturbation theory by assuming d large. There are two natural length scales associated with the confining potential $d_\pm = \hbar/\sqrt{2mV_\pm}$ so that we expand in the small parameters $d_\pm/d$. Since all the energy scales are set by E_0, we find it useful to describe the spin-orbit coupling in terms of the parameters $\alpha_\pm = \lambda_\pm^2/d_\pm$, which have the dimensions of a length. The product $E_0\alpha_\pm/\hbar$ has the dimensions of a velocity and plays the role of the Rashba coupling parameter. In the following, we make an expansion to first order in $d_\pm/d$ and up to third order in $\alpha_\pm k = \hbar^2\lambda_\pm^2 k/(2mV_\pm)$. Requiring that the second expansion parameter be smaller than 1 yields the condition (15) for the validity of our calculation. For the eigenvalues of Eq. (23), we find

$$\epsilon_{n\mathbf{k}s} = E_0 n^2\left[1 - 2\frac{d_- + d_+}{d} + se_1 k + e_2 k^2 + se_3 k^3\right] \tag{26}$$

and the eigenfunctions

$$f_{n\mathbf{k}s}(z) = c_{n\mathbf{k}s}\sin\left[\frac{n\pi}{d + \frac{d_-}{1-\alpha_- ks} + \frac{d_+}{1+\alpha_+ ks}} \times \left(\frac{d}{2} + z + \frac{d_-}{1 - \alpha_- ks}\right)\right], \tag{27}$$

with $n = 1, 2, \ldots$, where

$$c_{n\mathbf{k}s} = \sqrt{\frac{4}{d_e[2 - (se_1 k + e_2 k^2 + se_3 k^3)]}},$$
$$d_e = d + d_+ + d_-;$$
$$e_1 = 2\left(\frac{d_+}{d}\alpha_+ - \frac{d_-}{d}\alpha_-\right), \quad e_2 = -2\left(\frac{d_+}{d}\alpha_+^2 + \frac{d_-}{d}\alpha_-^2\right),$$
$$e_3 = 2\left(\frac{d_+}{d}\alpha_+^3 - \frac{d_-}{d}\alpha_-^3\right). \tag{28}$$

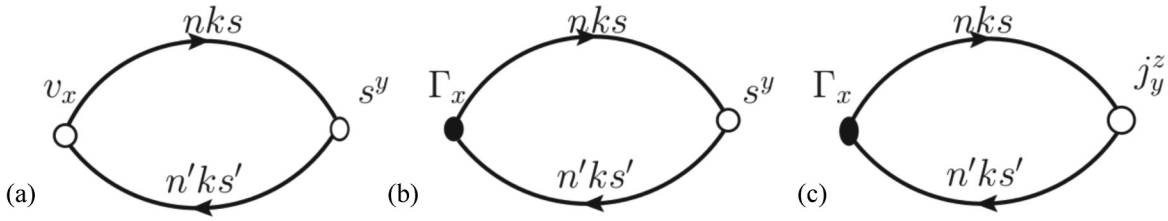

FIG. 2. Feynman bubble diagram for the EC [(a) and (b)] and SHC (c). The empty right dot indicates the spin density (EC) or the spin current density (SHC) bare vertex, the left empty one indicates the normal velocity operator, and the full dot is the dressed charge current density vertex.

Notice that the sign of the coefficients e_1 and e_3 depends on the relative strength of the spin-orbit coupling $\lambda_\pm$ and barrier heights $V_\pm$. To avoid trouble with negative signs in the following calculations, we assume that the couplings are labeled in such a way that $\lambda_+ > \lambda_-$, and $V_+ > V_-$ so that $e_1, e_3 > 0$.

In the next section, we evaluate the SHC assuming that $n = n_c$ is the topmost occupied subband. We use units such that $\hbar = c = 1$.

III. SPIN HALL CONDUCTIVITY

The SHC is defined as the nonequilibrium spin current density response to an applied electric field. By using a vector gauge with the electric field given by $\mathbf{E} = -\partial_t \mathbf{A}$, the Kubo formula, corresponding to the bubble diagram of Fig. 2, reads as

$$\sigma^{\rm SHE} = \lim_{\omega\to 0} \frac{{\rm Im}\langle\langle j_y^z; j_x\rangle\rangle}{\omega}, \tag{29}$$

where we have introduced the spin current operator $j_y^z = \sigma_z k_y/2m$ and the charge current operator $j_x = -e\hat{v}_x$. The number current operator, besides the standard velocity component, includes a spin-orbit-induced anomalous contribution $\hat{v}_x = k_x/m + \hat{\Gamma}_x$. Without vertex corrections, the anomalous contribution reads as

$$\hat{\Gamma}_x = \delta\hat{v}_x = [\lambda_+^2 V_+ \delta(z - z_+) - \lambda_-^2 V_- \delta(z - z_-)]\sigma_y. \tag{30}$$

This expression can be written in terms of the exact Green's functions and vertices as

$$\sigma^{\rm SHE} = -\lim_{\omega\to 0} {\rm Im}\frac{e}{\omega} \sum_{nn'\mathbf{k}\mathbf{k}'ss'} \langle n'\mathbf{k}'s'|\hat{v}_x|n\mathbf{k}s\rangle\langle n\mathbf{k}s|j_y^z|n'\mathbf{k}'s'\rangle \times \int_{-\infty}^{\infty} \frac{d\epsilon}{2\pi} G_{ns}(\epsilon_+,\mathbf{k}) G_{n's'}(\epsilon_-,\mathbf{k}'), \tag{31}$$

where $e > 0$ is the unit charge, $\epsilon_\pm = \epsilon \pm \omega/2$, and $G_{ns}(\epsilon,\mathbf{k}) = (\epsilon - E_{n\mathbf{k}s} + {\rm isgn}\epsilon/2\tau)^{-1}$ is the Green's function averaged over disorder in the self-consistent Born approximation with self-energy

$$\Sigma_{ns}(\mathbf{r},\mathbf{r}';\epsilon) = \frac{\delta(\mathbf{r}-\mathbf{r}')}{2\pi N_0 \tau} G_{ns}(\mathbf{r},\mathbf{r};\epsilon). \tag{32}$$

After performing the integral over the frequency, we obtain

$$\sigma^{\rm SHE} = -\frac{e}{2\pi} \sum_{nn'\mathbf{k}ss'} \langle n'\mathbf{k}s'|\hat{v}_x|n\mathbf{k}s\rangle\langle n\mathbf{k}s|j_y^z|n'\mathbf{k}s'\rangle G^R_{n\mathbf{k}s} G^A_{n'\mathbf{k}s'}, \tag{33}$$

where we have introduced the retarded and advanced zero-energy Green's functions at the Fermi level

$$G^{R,A}_{n\mathbf{k}s} = \frac{1}{-E_{n\mathbf{k}s} + \mu \pm {\rm i}/2\tau} \tag{34}$$

and exploited the fact that plane waves at different momentum $\mathbf{k}$ are orthogonal.

To proceed further, we need the expression for the vertices. It is easy to recognize that the standard part of the velocity operator k_x/m does not contribute since it requires $s = s'$, whereas the matrix elements of j_y^z differ from zero only for $s \neq s'$. Explicitly, we have

$$\langle n'\mathbf{k}s'|k_x|n\mathbf{k}s\rangle = k_x\langle f_{n'\mathbf{k}s'}|f_{n\mathbf{k}s}\rangle\delta_{s's} = \langle f_{n'\mathbf{k}s'}|f_{n\mathbf{k}s}\rangle k\cos\theta_{\mathbf{k}}\,\delta_{s's}, \tag{35}$$

$$\langle n\mathbf{k}s'|\delta\hat{v}_x|n\mathbf{k}s\rangle = (\cos\theta_{\mathbf{k}}\,\sigma_{z,s's} + \sin\theta_{\mathbf{k}}\,\sigma_{y,s's}) \times \frac{\Delta E_{nk}}{k}\langle f_{n\mathbf{k}s'}|f_{n\mathbf{k}s}\rangle, \tag{36}$$

$$\langle n\mathbf{k}s|j_y^z|n'\mathbf{k}s'\rangle = \langle f_{n\mathbf{k}s}|f_{n'\mathbf{k}s'}\rangle\frac{k}{2m}\sin\theta_{\mathbf{k}}\,\sigma_{x,ss'}, \tag{37}$$

where $\Delta E_{nk} = (E_{nk+} - E_{nk-})/2 = E_0 n^2(e_1 k + e_3 k^3)$ is half the spin-splitting energy in the nth band. Equation (36) is straightforwardly obtained from the eigenvalue equation (23) for the functions $f_{n\mathbf{k}s}(z)$.

Let us now discuss the overlaps between the wave functions $\langle f_{n\mathbf{k}s}|f_{n'\mathbf{k}'s'}\rangle$. If $n = n'$ we have

$$\langle f_{n\mathbf{k}s}|f_{n\mathbf{k}'s'}\rangle = \frac{d_e}{2} c_{nks} c_{nk's'}\left[1 - \frac{e_1(ks + k's') + e_2(k^2 + k'^2) + e_3(k^3 s + k'^3 s')}{4}\right], \tag{38}$$

which is unity plus corrections of order $(d_\pm/d)$ when $s,k \neq s',k'$. If $n \neq n'$, $\langle f_{n\mathbf{k}s}|f_{n'\mathbf{k}'s'}\rangle$ is at least of order $(d_\pm/d)$. Before continuing our calculation we observe that it is important to distinguish between the intraband ($n = n'$) and the interband ($n \neq n'$) contributions. The interband contributions are of second order in $d_\pm/d$ because they are proportional to $\langle f_{n\mathbf{k}s}|f_{n'\mathbf{k}'s'}\rangle^2$. Since we limit our expansion to the first order in $d_\pm/d$, we will from now on neglect these contributions.

Notice, however, that this approximation is no longer valid when the intraband splitting controlled by e_1 and e_3 vanishes. In this case, one can not avoid taking into account the interband contributions. In the same spirit, we also approximate the intraband overlap $\langle f_{n\mathbf{k}s}|f_{n\mathbf{k}'s'}\rangle \simeq 1$ because all of our results are at least linear in $(d_\pm/d)$ and we neglect higher-order terms.

The anomalous contribution to the velocity vertex $\hat{\Gamma}_x$ can be computed following the procedure described in Ref. [37] according to the equations (see Fig. 3)

$$\begin{aligned}\hat{\Gamma}_x &= \tilde{\gamma}_x + \frac{1}{2\pi N_0\tau}\sum_{\mathbf{k}'} G^R_{\mathbf{k}'}\hat{\Gamma}_x G^A_{\mathbf{k}'},\\ \tilde{\gamma}_x &= \hat{\delta}v_x + \frac{1}{2\pi N_0\tau}\sum_{\mathbf{k}'} G^R_{\mathbf{k}'}\,\frac{k'_x}{m}\,G^A_{\mathbf{k}'} \equiv \tilde{\gamma}^{(1)} + \tilde{\gamma}^{(2)}.\end{aligned} \tag{39}$$

To extend the treatment to the present case, the projection must be made over the states $|n\mathbf{k}s\rangle$. Assuming that the impurity potential does not depend on z, the matrix elements of the effective vertex $\tilde{\gamma}^{(2)}$ are

$$\begin{aligned}\gamma^{(2)nn}_{ss'}(k) &\equiv \langle n\mathbf{k}s|\tilde{\gamma}^{(2)}|n\mathbf{k}s'\rangle\\ &= \frac{1}{2\pi N_0\tau}\sum_{n_1\mathbf{k}'s_1}\langle n\mathbf{k}s|n_1\mathbf{k}'s_1\rangle G^R_{n_1\mathbf{k}'s_1}\\ &\quad\times\frac{k'_x}{m}\,G^A_{n_1\mathbf{k}'s_1}\langle n_1\mathbf{k}'s_1|n\mathbf{k}s'\rangle,\end{aligned} \tag{40}$$

and $\gamma^{(1)nn}_{ss'}(k) \equiv \langle n\mathbf{k}s|\tilde{\gamma}^{(1)}|n\mathbf{k}s'\rangle$ is given by Eq. (36). The matrix elements $\langle n\mathbf{k}s|n_1\mathbf{k}'s_1\rangle$ and $\langle n_1\mathbf{k}'s_1|n\mathbf{k}s'\rangle$ are those of the impurity potential:

$$\langle n\mathbf{k}s|n_1\mathbf{k}'s_1\rangle = \tfrac{1}{2}\langle f_{n\mathbf{k}s}|f_{n_1\mathbf{k}'s_1}\rangle[1+ss_1e^{\mathrm{i}(\theta_{\mathbf{k}'}-\theta_{\mathbf{k}})}], \tag{41}$$

$$\langle n_1\mathbf{k}'\lambda_1|n\mathbf{k}s'\rangle = \tfrac{1}{2}\langle f_{n_1\mathbf{k}'s_1}|f_{n\mathbf{k}s'}\rangle[1+s's_1e^{-\mathrm{i}(\theta_{\mathbf{k}'}-\theta_{\mathbf{k}})}]. \tag{42}$$

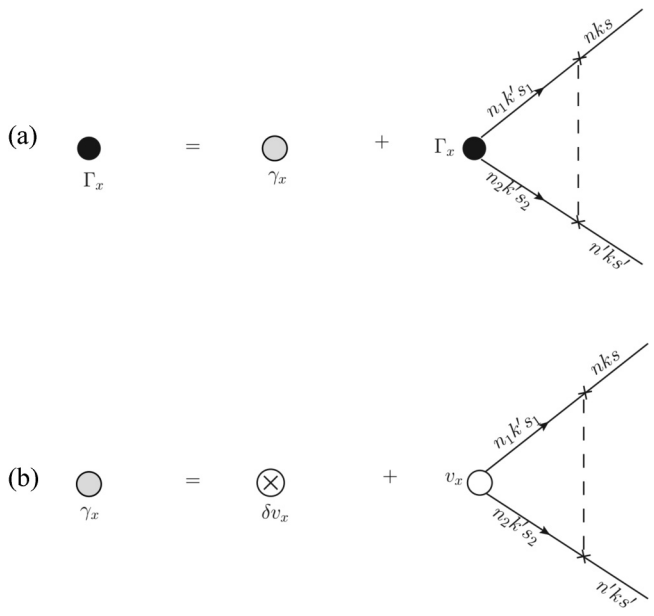

FIG. 3. Ladder resummation for the spin-dependent part of the dressed charge current density vertex. The dashed line represents the correlation between propagators scattering off the same impurity site.

By observing that $k'_x = k'\cos\theta_{\mathbf{k}'}$, one can perform the integration over the direction of $\mathbf{k}'$ in the expression of $\gamma^{(2)nn}_{ss'}(k)$,

$$\begin{aligned}&\frac{1}{4}\int_0^{2\pi}\frac{d\theta_{\mathbf{k}'}}{2\pi}[1+ss_1e^{\mathrm{i}(\theta_{\mathbf{k}'}-\theta_{\mathbf{k}})}]\cos\theta_{\mathbf{k}'}\,[1+s's_1e^{-\mathrm{i}(\theta_{\mathbf{k}'}-\theta_{\mathbf{k}})}]\\ &\quad= \frac{s_1}{8}[se^{-\mathrm{i}\theta_{\mathbf{k}}}+s'e^{\mathrm{i}\theta_{\mathbf{k}}}],\end{aligned} \tag{43}$$

to get

$$\begin{aligned}\gamma^{(2)nn}_{ss'}(k) &= \frac{(\cos\theta_{\mathbf{k}}\,\sigma_{z,ss'}+\sin\theta_{\mathbf{k}}\,\sigma_{y,ss'})}{16\pi N_0\tau}\sum_{n_1\mathbf{k}'s_1}s_1\langle f_{n\mathbf{k}s}|f_{n_1\mathbf{k}'s_1}\rangle\\ &\quad\times\langle f_{n_1\mathbf{k}'s_1}|f_{n\mathbf{k}s'}\rangle G^R_{n_1\mathbf{k}'s_1}\,\frac{k'}{m}\,G^A_{n_1\mathbf{k}'s_1}.\end{aligned} \tag{44}$$

Approximating $\langle f_{n\mathbf{k}s}|f_{n_1\mathbf{k}'s_1}\rangle \sim \delta_{nn_1}$, summing over s_1, and integrating over k with the technique shown in the Appendix yields

$$\gamma^{(2)nn}_{ss'}(k) = -(\cos\theta_{\mathbf{k}}\,\sigma_{z,ss'}+\sin\theta_{\mathbf{k}}\,\sigma_{y,ss'})E_0n^2\big(e_1+2e_3k^2_{Fn}\big), \tag{45}$$

where we have introduced the spin-averaged Fermi momentum in the nth subband

$$\frac{k^2_{Fn}}{2m} = \mu - E_0n^2. \tag{46}$$

On the other hand, $\gamma^{(1)nn}_{ss'}(k)$ is given by

$$\gamma^{(1)nn}_{ss'}(k) = (\cos\theta_{\mathbf{k}}\,\sigma_{z,ss'}+\sin\theta_{\mathbf{k}}\,\sigma_{y,ss'})E_0n^2\big(e_1+e_3k^2_{Fn}\big), \tag{47}$$

where k has been replaced by k_{Fn} at the required level of accuracy. Combining $\gamma^{(1)nn}_{ss'}(k)$ and $\gamma^{(2)nn}_{ss'}(k)$ as mandated by Eq. (39), we finally obtain

$$\gamma^{nn}_{x,ss'}(k) = -(\cos\theta_{\mathbf{k}}\,\sigma_{z,ss'}+\sin\theta_{\mathbf{k}}\,\sigma_{y,ss'})E_0n^2e_3k^2_{Fn}\,. \tag{48}$$

Next, we project the equation for the vertex corrections in the basis of the eigenstates and get the following integral equation:

$$\begin{aligned}\Gamma^{nn}_{x,ss'}(k) &= \gamma^{nn}_{x,ss'}(k) + \frac{1}{2\pi N_0\tau}\sum_{n_1n_2\mathbf{k}'s_1s_2}\langle n\mathbf{k}s|n_1\mathbf{k}'s_1\rangle\\ &\quad\times G^R_{n_1\mathbf{k}'s_1}\Gamma^{n_1n_2}_{x,s_1s_2}(k')G^A_{n_2\mathbf{k}'s_2}\langle n_2\mathbf{k}'s_2|n\mathbf{k}s'\rangle,\end{aligned} \tag{49}$$

which, by confining to intraband processes only, can be solved with the ansatz $\Gamma^{nn}_{x,ss'}(k) = \Gamma^n(k_{Fn})[\cos(\theta_{\mathbf{k}})(\sigma_z)_{ss'} + \sin(\theta_{\mathbf{k}})(\sigma_y)_{ss'}]$ yielding

$$\Gamma^{nn}_{x,ss'}(k) = \gamma^{nn}_{x,ss'}(k)\frac{\tau^{(n)}_{\mathrm{DP}}}{\tau}. \tag{50}$$

By performing the integral over momentum and summing over the spin indices in Eq. (33), one obtains the SHC as

$$\sigma^{\mathrm{SHE}} = \sum_{n=1}^{n_c}\frac{e}{8\pi}\frac{2\tau}{\tau^{(n)}_{\mathrm{DP}}}\frac{\Gamma^n(k_{Fn})}{\Delta E_{nk_{Fn}}/k_{Fn}}, \tag{51}$$

where n_c is the number of occupied bands.

If vertex corrections are ignored, i.e., if we approximate $\Gamma^n(k_{Fn}) = \Delta E_{nk_{Fn}}/k_{Fn}$ [cf. Eq. (36)], Eq. (51) gives us

$$\sigma^{\rm SHE}_{\rm drift} = \sum_{n=1}^{n_c} \frac{e}{8\pi}\frac{2\tau}{\tau^{(n)}_{\rm DP}}, \tag{52}$$

which, in the weak disorder limit ($\tau \to \infty$), reproduces the result of Ref. [41], i.e., $\sigma^{\rm SHE}_{\rm drift} = (e/8\pi)n_c$.

If instead the renormalized vertex (50) is properly taken into account, we obtain

$$\sigma^{\rm SHE} = -\sum_{n}^{n_c} \frac{e}{4\pi}\frac{e_3 k_{Fn}^2}{e_1 + e_3 k_{Fn}^2}. \tag{53}$$

Notice that, being proportional to $\lambda_\pm^4$ ($e_1 \propto \lambda_\pm^2$, $e_3 \propto \lambda_\pm^6$), this result is consistent with the result obtained in Ref. [40] for a different but related model. Making use of the explicit expressions for e_1 and e_3, we finally get the previously reported result of Eq. (10).

IV. EDELSTEIN CONDUCTIVITY

In the dc limit, i.e., for $\omega \to 0$, the Edelstein conductivity (EC) is defined by

$$\sigma^{\rm EE} = \lim_{\omega\to 0} \frac{{\rm Im}\langle\langle s^y; j_x\rangle\rangle}{\omega}. \tag{54}$$

That can be written as

$$\sigma^{\rm EE} = -\lim_{\omega\to 0}{\rm Im}\frac{e}{\omega}\sum_{nn'\mathbf{k}\mathbf{k}'ss'}\langle n'\mathbf{k}'s'|\hat{v}_x|n\mathbf{k}s\rangle\langle n\mathbf{k}s|s^y|n'\mathbf{k}'s'\rangle \times \int_{-\infty}^{\infty}\frac{d\epsilon}{2\pi}G_{ns}(\epsilon_+,\mathbf{k})G_{n's'}(\epsilon_-,\mathbf{k}'). \tag{55}$$

After performing the integral over frequency we get

$$\sigma^{\rm EE} = -\frac{e}{2\pi}\sum_{nn'\mathbf{k}ss'}\langle n'\mathbf{k}s'|\hat{v}_x|n\mathbf{k}s\rangle\langle n\mathbf{k}s|s^y|n'\mathbf{k}s'\rangle G^R_{n\mathbf{k}s}G^A_{n'\mathbf{k}s'}, \tag{56}$$

where we have used again the orthogonality of the eigenvectors with different momentum. As shown in Fig. 2, we consider the bare vertex for the spin density $s^y = \sigma_y/2$ and the two vertices for the number current density $\hat{v}_x = \hat{\Gamma}_x + k_x/m$ [37], $\hat{\Gamma}_x$ being the renormalized spin-dependent part of the vertex. Clearly, the two parts of the number current vertex yield two separate contributions to the EC and we are now going to evaluate them separately. We then evaluate Fig. 2(a) as

$$\sigma^{{\rm EE},(a)} = -\frac{e}{4\pi m}\sum_{nn'\mathbf{k}ss'}\langle n'\mathbf{k}s'|k_x|n\mathbf{k}s\rangle \times \langle n\mathbf{k}s|\sigma_y|n'\mathbf{k}s'\rangle G^R_{n\mathbf{k}s}G^A_{n'\mathbf{k}s'}, \tag{57}$$

where the matrix elements of the spin vertex are

$$\langle n\mathbf{k}s|\sigma_y|n'\mathbf{k}s'\rangle = \langle f_{n\mathbf{k}s}|f_{n'\mathbf{k}s'}\rangle(\cos\theta_{\mathbf{k}}\,\sigma_{z,ss'} - \sin\theta_{\mathbf{k}}\,\sigma_{y,ss'}). \tag{58}$$

Setting $n' = n$ and using Eq. (26) for the energy eigenvalues, we can perform the integration over the momentum in Eq. (57) obtaining for $\sigma^{{\rm EE},(a)}$ the expression

$$\sigma^{{\rm EE},(a)} = \sum_{n=1}^{n_c} eN_0\tau E_0 n^2\left(e_1 + 2e_3 k_{Fn}^2\right). \tag{59}$$

Next, we evaluate Fig. 2(b) as

$$\sigma^{{\rm EE},(b)} = -\frac{e}{4\pi}\sum_{nn'\mathbf{k}ss'}\langle n'\mathbf{k}s'|\hat{\Gamma}_x|n\mathbf{k}s\rangle\langle n\mathbf{k}s|\sigma_y|n'\mathbf{k}s'\rangle \times G^R_{n\mathbf{k}s}G^A_{n'\mathbf{k}s'}, \tag{60}$$

We set $n = n'$ and insert the result obtained in Eq. (50) for $\langle n\mathbf{k}s'|\hat{\Gamma}_x|n\mathbf{k}s\rangle$. Since both the matrix elements of $\hat{\Gamma}_x$ and σ_y contain terms proportional to $\cos(\theta_{\mathbf{k}})$ and $\sin(\theta_{\mathbf{k}})$, we must distinguish between $s = s'$ [first term in Eq. (48)] and $s \neq s'$ [second term in Eq. (48)]. If $s = s'$ we have

$$\sigma_1^{{\rm EE},(b)} = -\frac{e}{4\pi}\sum_{n\mathbf{k}s}\langle ns|\tilde{\Gamma}_x|n\mathbf{k}s\rangle\langle n\mathbf{k}s|\sigma_y|n\mathbf{k}s\rangle G^R_{n\mathbf{k}s}G^A_{n\mathbf{k}s}. \tag{61}$$

The integral over the momentum can be done with the technique shown in the Appendix to yield

$$\sigma_1^{{\rm EE},(b)} = \sum_{n}^{n_c} eN_0\tau E_0 n^2 e_3 k_{Fn}^2\frac{\tau^{(n)}_{\rm DP}}{2\tau}. \tag{62}$$

If $s \neq s'$, we have instead

$$\sigma_2^{{\rm EE},(b)} = -\frac{e}{4\pi}\sum_{n\mathbf{k}s}\langle n\mathbf{k}\bar{s}|\tilde{\Gamma}_x|n\mathbf{k}s\rangle\langle n\mathbf{k}s|\sigma_y|n\mathbf{k}'\bar{s}\rangle G^R_{n\mathbf{k}s}G^A_{n\mathbf{k}\bar{s}}. \tag{63}$$

So, we can conclude that

$$\sigma_2^{{\rm EE},(b)} = \sum_{n=1}^{n_c} eN_0\tau E_0 n^2\frac{e_3 k_{Fn}^2}{\left(2\tau\Delta E_{nk_{Fn}}\right)^2} \tag{64}$$

with $\Delta E_{nk_{Fn}}$ defined in Eq. (12). Combining the (a) and (b) contributions, the final result for the Edelstein conductivity is found to be

$$\sigma^{\rm EE} = \sum_{n=1}^{n_c} eN_0\tau E_0 n^2\left[e_1 + 3e_3 k_{Fn}^2 + \frac{2e_3 k_{Fn}^2}{\left(2\tau\Delta E_{nk_{Fn}}\right)^2}\right], \tag{65}$$

which is easily seen to be equivalent to Eq. (11).

V. DISCUSSION

The two central results (65) and (53) may be interpreted along the lines outlined in the Introduction. We begin by noticing that both conductivities are expressed as simple sums of independent subband contributions, hence, the relation (8) is valid separately within each subband. The second step is the identification of the quantity $\tau_s/L_{\rm so}$ for a given subband. Clearly, τ_s must be identified with the Dyakonov-Perel relaxation time $\tau^{(n)}_{\rm DP}$ defined in (14). For the spin-orbit length $L_{\rm so}$, one notices that the quantity $2\alpha p_F$ in the Rashba model corresponds to the band splitting, and hence must here be replaced by $2\Delta E_{nk_{Fn}}$. This yields, after restoring $\hbar$ in the following,

$$L^{(n)}_{\rm so} = \frac{\hbar v_{Fn}}{2\Delta E_{nk_{Fn}}}, \tag{66}$$

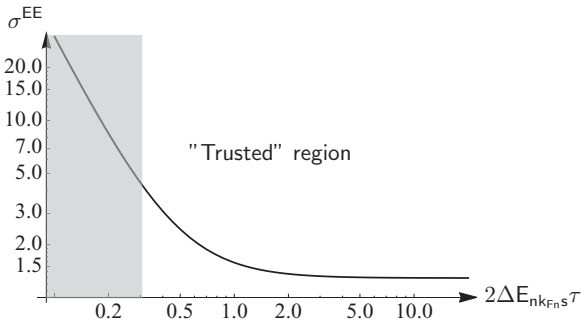

FIG. 4. Value of the EC in units of the "normal" values $eN_0\alpha\tau$ as a function of $2\Delta E_{nk_{Fn}s}\tau$. In our model α corresponds to $E_0n^2(e_1 + e_3k_{Fn}^2)$. The value of τ is fixed, and we can see the dependence of the EC on the spin-splitting energy. Notice that the curve can not be trusted in the extreme diffusive limit $2\Delta E_{nk_{Fn}}\tau \ll 1$ since, in this regime, additional relaxation mechanisms due to interband effects arise (cf. discussion at the end of the section) and the divergence of the enhancement is stopped. The gray area estimates the region where interband corrections are expected to become progressively more relevant.

i.e., $\tau_s/L_{\rm so} \to \tau_{\rm DP}^{(n)}/L_{\rm so}^{(n)}$. With this prescription one can apply Eq. (8) subband by subband and obtain

$$\sigma^{{\rm EE},(n)} = \frac{\tau_{\rm DP}^{(n)}}{L_{\rm so}^{(n)}}\left[\sigma^{{\rm SHE},(n)} - \sigma_{\rm drift}^{{\rm SHE},(n)}\right], \tag{67}$$

where $\sigma^{{\rm SHE},(n)}, \sigma_{\rm drift}^{{\rm SHE},(n)}$ stand for the nth band contributions to Eqs. (53) and (52), respectively. It is now immediate to see that a sum over the subbands leads to the EC of Eq. (65). We may thus conclude the following: a nonvanishing SHC in the presence of Rashba spin-orbit coupling gives rises to an anomalous EC scaling with the inverse scattering time; conversely, an anomalous EC yields a nonvanishing SHC.

Some experimental studies [47,48] show that devices of the type shown in Fig. 1 could present giant spin-orbit coupling. Following Ref. [47], a metallic film of 10 monatomic layers of Al ($d \approx 1$ nm) shows a large spin-splitting energy of $\Delta E_{nk_{Fn}} = 240$ meV in the second band ($n = 2$). Introducing these values in our model, with a barrier of $V \approx 4$ eV, one can find a value for $\lambda \approx 4.9 \times 10^{-9}$ cm. We should remember that in this experiment there is only one interfacial barrier (the other barrier is the vacuum) so we will assume that only λ_+ survives. With these values, one obtains $\sigma^{\rm SHE} \approx -0.29 \times e/(8\pi)$ which seems an encouraging result. In Fig. 4, we report the EC in units of the "normal" value as a function of $2\Delta E_{nk_{Fn}}\tau$.

We now consider two physically interesting limiting cases of the general solution:

(1) the insulator-metal-vacuum junction $\lambda_- \ll \lambda_+ \equiv \lambda$, $V_- \gg V_+ \equiv V$;

(2) films with the same spin-orbit constant coupling at the two interfaces $\lambda_- = \lambda_+ = \lambda$.

In the first case, we get

$$\sigma^{\rm EE} = \sum_n^{n_c} \frac{2eN_0\tau E_0 n^2\lambda^2}{d\hbar}\left(1 + \frac{\hbar^2\pi^2 V}{8\tau^2 E_0^3 n^4}\right), \tag{68}$$

$$\sigma^{\rm SHE} = -\sum_n^{n_c} \frac{e}{4\pi\hbar^3} 2mk_{Fn}^2 V\lambda^4. \tag{69}$$

There are some experimental studies of metal-metal-vacuum junctions that show giant spin-orbit coupling [47] and where one could test the prediction of Eqs. (68) and (69). Although Eq. (69) is obtained for small values of the parameter $2mk_{Fn}^2 V\lambda^4/\hbar^2 \ll 1$, the structure of the result is quite interesting: it suggests that this kind of device, the insulator-metal-vacuum junction, could be an efficient spintronic device, its transport properties being proportional to the barrier height V.

In the second case, let us first assume a "quasisymmetric" configuration, i.e., although $\lambda_+ = \lambda_- \equiv \lambda$, the barrier heights are different $V_+ \neq V_-$. We then obtain that the spin splitting of the bands vanishes to linear order in k ($e_1 = 0$) (see footnote 3) so that

$$\sigma^{\rm SHE} = -\sum_n^{n_c} \frac{e}{4\pi\hbar} \tag{70}$$

and

$$\sigma^{\rm EE} = \sum_n^{n_c} eN_0\tau\frac{\Delta E_{nk_{Fn}}}{k_{Fn}\hbar}\left[3 + \frac{\hbar^2}{2\left(\tau\Delta E_{nk_{Fn}}\right)^2}\right]. \tag{71}$$

The SHC in this limit is independent of λ. This very striking result is reminiscent of the universal result $\frac{e}{8\pi\hbar}$ obtained for a single Bychkov-Rashba band when vertex corrections are ignored [4]. However, vertex corrections are now fully included, yet the SHC is not only finite, but *independent* of λ and equal to the single-band universal result multiplied by a factor -2! We emphasize that this result has nothing to do with the nonvanishing intrinsic SHC that arises in certain generalized models of spin-orbit coupling with winding number higher than 1 [49]. Rather, it has everything to do with the k dependence of the transverse subbands describing the electron wave function in the z direction. We also find that the anomalous part of the Edelstein effect becomes large, as it is proportional to $1/\Delta E_{nk_{Fn}}$, and the splitting vanishes with the third power of k at small k.

Let us finally discuss the fully inversion-symmetric limit of the model $\lambda_+ = \lambda_-$ and $V_+ = V_-$. We notice that in this case the limit of Eq. (53) does not exist because both e_1 and e_3 vanish (the spin splitting is identically zero!), while the value of Eq. (53) depends on the order in which e_1 and e_3 tend to zero, in particular on whether they tend to zero simultaneously, or e_1 tend to zero before e_3, as in the "quasisymmetric" case above. The origin of this apparently unphysical nonanalytic behavior can be traced back to the singular character of the vertex (50) for vanishing spin splitting. Under these circumstances, the Dyakonov-Perel spin relaxation time (14) diverges, apparently implying spin conservation. However, even in the inversion-symmetric limit, interband effects provide spin relaxation processes which regularize the vertex. Such effects are typically negligible away from the inversion-symmetric limit since they are proportional to the square of the wave-function overlap between different bands and therefore scale as $(d_\pm/d)^2$. However, in the inversion-symmetric limit, they can not be neglected.

A full analysis of interband effects is beyond the scope of this paper, and we limit ourselves to a heuristic discussion of the physical origin of the spin relaxation mechanism due to interband virtual transitions. In the inversion-symmetric limit, the Hamiltonian is invariant upon the simultaneous operations of space inversion along the z axis ($z \to -z$) and helicity

flipping ($s \to -s$), i.e., a full mirror reflection in the x-y plane. Hence, the eigenfunctions can be classified as even or odd under such a reflection:

$$f_{n\mathbf{k}s}(z) = P_n f_{n\mathbf{k}-s}(-z), \tag{72}$$

where $P_n = \pm 1$. Furthermore, the parity eigenvalue P_n is the same as in the absence of spin-orbit interaction because the reflection commutes with the spin-orbit interaction: $P_n = 1$ for odd n and $P_n = -1$ for even n.

Since states of opposite helicity are degenerate, one can construct, in each band n, states that are linear combinations of the helicity eigenstates $|\pm\rangle$. Among these, the two states of maximal spin polarization in the positive and negative z direction are

$$\psi_{n\mathbf{k}\uparrow} = \tfrac{1}{2}[f_{n\mathbf{k}+}(z)|+\rangle + f_{n\mathbf{k}-}(z)|-\rangle], \tag{73}$$

$$\psi_{n\mathbf{k}\downarrow} = \tfrac{1}{2}[f_{n\mathbf{k}+}(z)|+\rangle - f_{n\mathbf{k}-}(z)|-\rangle]. \tag{74}$$

That these are states of maximal polarization can be seen by expressing them in terms of the eigenstates $|\uparrow\rangle$ and $|\downarrow\rangle$ of σ_z:

$$\psi_{n\mathbf{k}\uparrow} = \frac{f_{n\mathbf{k}+}(z) + f_{n\mathbf{k}-}(z)}{2}|\uparrow\rangle + ie^{i\theta_{\mathbf{k}}}\frac{f_{n\mathbf{k}+}(z) - f_{n\mathbf{k}-}(z)}{2}|\downarrow\rangle, \tag{75}$$

$$\psi_{n\mathbf{k}\downarrow} = \frac{f_{n\mathbf{k}+}(z) - f_{n\mathbf{k}-}(z)}{2}|\uparrow\rangle + ie^{i\theta_{\mathbf{k}}}\frac{f_{n\mathbf{k}+}(z) + f_{n\mathbf{k}-}(z)}{2}|\downarrow\rangle. \tag{76}$$

When the spin-orbit interaction is weak, one has $f_{n\mathbf{k}+}(z) \simeq f_{n\mathbf{k}-}(z)$ so the first state is almost entirely "up" and the second one is almost entirely "down." One sees immediately that, within the first Born approximation, impurity scattering can not produce spin flipping within a band characterized by a certain value of n because the matrix element of the z-independent disorder potential between $\psi_{n\mathbf{k}\uparrow}$ and $\psi_{n\mathbf{k}'\downarrow}$ vanishes by virtue of Eq. (72). Thus, the ordinary Elliot-Yafet mechanism of spin relaxation is absent in this model.

On the other hand, spin flipping may occur in the second Born approximation by going through an intermediate state in a band of opposite parity. For example, an electron may first jump, under the action of the disorder potential, to a state of *opposite* spin in an unoccupied band of opposite parity; then, in a second step it may return to the original band without flipping its spin. Alternatively, the spin may remain unchanged in the transition to the unoccupied band, and flip on the way back to the original band. As a result of such processes, and of possible subtle interference effects between them, a new mechanism of spin relaxation arises, which we call *interband spin relaxation*, with rate τ_{IB}^{-1}.

We may estimate its order of magnitude by considering that it must be controlled by the ratio of the momentum relaxation rate $\sim 1/\tau$ and the interband energy separation E_{IB}. Hence, in second-order perturbation theory in the small effective expansion parameter $1/E_{\mathrm{IB}}\tau$ [cf. Eq. (16)], we expect $\gamma_{\mathrm{IB}} \sim (1/\tau)(E_{\mathrm{IB}}\tau)^{-2} \sim \tau^{-3}$. This is different from the standard Elliott-Yafet spin relaxation rate, which scales as $\sim\tau^{-1}$.

When this additional relaxation mechanism is taken into account, the diverging DP relaxation time in Eq. (50) for the vertex is replaced by the finite total spin relaxation time $(\tau_{\mathrm{DP}}^{-1} + \tau_{\mathrm{IB}}^{-1})^{-1}$. Thus, the nonanalyticity is cured.

The regime analyzed in this paper corresponds to the situation in which $\tau_{\mathrm{DP}}^{-1} \gg \tau_{\mathrm{IB}}^{-1}$, and interband spin relaxation can be neglected. The latter is expected to become relevant when $\tau_{\mathrm{DP}}^{-1} \sim \tau_{\mathrm{IB}}^{-1}$, which means $\Delta E_{nk_{Fn}s}\tau \sim (E_{\mathrm{IB}}\tau)^{-1} \sim 0.1$. Clearly, when looking at the fully symmetric limit, with vanishing spin splitting, interband relaxation must be taken into account, together with interband contributions to the SHC and EC. Once more, a full-fledged treatment of this regime is beyond the scope of this work.

VI. CONCLUSIONS

We have developed a simple model for describing spin transport effects and spin-charge conversion in heterostructures consisting of a metallic film sandwiched between two different insulators. All the effects we have considered depend crucially on the three-dimensional nature of the system, in particular, the fact that the transverse wave functions depend on the in-plane momentum, and on the lack of inversion symmetry caused by the different properties of the top and bottom metal-insulator interfaces, each characterized by a different barrier height (gap) and spin-orbit coupling strength. After a careful consideration of vertex corrections, we find that the model supports a nonzero intrinsic SHC, in sharp contrast to the 2DEG Rashba case. Strikingly, in a "quasisymmetric" junction, the SHC reaches a maximal and universal value. We have also calculated the Edelstein effect for the same model and found that the induced spin polarization is the sum of two different contributions. The first one is analogous to the term found in the 2DEG Rashba case, whereas the second "anomalous" one has a completely different nature. Namely, it is inversely proportional to the scattering time, indicating that it is caused by the combined action of multiple electron-impurity scattering and spin-orbit coupling. We have also discussed the general connection between the nonvanishing SHC and the anomalous term in the EC. Furthermore, by Onsager's reciprocity relations, our results are immediately relevant to the inverse Edelstein effect [34,42,50], in which a nonequilibrium spin density induces a charge current. The above features, although discussed here for a specific model, are expected to be general, proper to any nonstrictly two-dimensional system in which the spin-orbit interaction is nonhomogeneous across the confining direction. Technical applications of this idea could lead to a new class of spin-orbit-coupling-based devices.

ACKNOWLEDGMENTS

C.G. acknowledges support by CEA through the DSM-Energy Program (Project No. E112-7-Meso-Therm-DSM). G.V. acknowledges support from NSF Grant No. DMR-1104788.

APPENDIX: INTEGRALS OF GREEN'S FUNCTIONS

To perform the integral of Eq. (57), we exploit the poles with the Cauchy theorem of residues. We use the formulas [37]

$$\sum_{\mathbf{k}} G^R_{n\mathbf{k}s} G^A_{n\mathbf{k}s} f(\mathbf{k}) = 2\pi N_{ns} \tau f(k_{Fns}), \tag{A1}$$

$$\sum_{\mathbf{k}} G^R_{n\mathbf{k}-} G^A_{n\mathbf{k}+} f(\mathbf{k}) = \frac{2\pi N_0 \tau}{1 - i2\tau \Delta E_{nk_{F_n}}} f(k_{F_n}), \tag{A2}$$

where $f(\mathbf{k})$ is assumed to be regular, N_{ns} is the density of states in the n subband, and k_{Fns} is the corresponding momentum. Following Ref. [40], the expression for both the density of states and the Fermi momentum can be obtained in terms of the coefficients of the energy eigenvalues expansion

$$k_{Fns} = k_{Fn} + E_0 n^2 \left[s\frac{e_1}{2} - \frac{e_1^2}{8k_{Fn}} - s\left(\frac{e_1 e_2}{2} - \frac{e_3 k_{Fn}^2}{2}\right)\right], \tag{A3}$$

$$N_{ns} = N_0 \left\{ 1 + E_0 n^2 \left[s\frac{e_1}{2k_{Fn}} - e_2 + s\left(\frac{e_1 e_2}{k_{Fn}} - \frac{3e_3 k_{Fn}}{2} - \frac{e_1^3}{16 k_{Fn}^3}\right)\right]\right\}. \tag{A4}$$

Hence, for instance,

$$\sum_{\mathbf{k}s} s G^R_{n\mathbf{k}s} G^A_{n\mathbf{k}s} k = 2\pi\tau \sum_s s k_{Fns} N_{ns} = E_0 n^2 (e_1 + 2e_3 k_{Fn}^2). \tag{A5}$$

[1] J. E. Hirsch, Phys. Rev. Lett. **83**, 1834 (1999).
[2] S. Zhang, Phys. Rev. Lett. **85**, 393 (2000).
[3] S. Murakami, N. Nagaosa, and S.-C. Zhang, Science **301**, 1348 (2003).
[4] J. Sinova, D. Culcer, Q. Niu, N. A. Sinitsyn, T. Jungwirth, and A. H. MacDonald, Phys. Rev. Lett. **92**, 126603 (2004).
[5] H.-A. Engel, E. I. Rashba, and B. I. Halperin, in *Handbook of Magnetism and Advanced Magnetic Materials*, Vol. V, edited by H. Kronmüller and S. Parkin (Wiley, Chichester, UK, 2007), pp. 2858–2877.
[6] R. Raimondi, C. Gorini, P. Schwab, and M. Dzierzawa, Phys. Rev. B **74**, 035340 (2006).
[7] D. Culcer and R. Winkler, Phys. Rev. B **76**, 245322 (2007).
[8] D. Culcer and R. Winkler, Phys. Rev. Lett. **99**, 226601 (2007).
[9] D. Culcer, E. M. Hankiewicz, G. Vignale, and R. Winkler, Phys. Rev. B **81**, 125332 (2010).
[10] W.-K. Tse, J. Fabian, I. Žutić, and S. Das Sarma, Phys. Rev. B **72**, 241303 (2005).
[11] V. M. Galitski, A. A. Burkov, and S. Das Sarma, Phys. Rev. B **74**, 115331 (2006).
[12] T. Tanaka and H. Kontani, New J. Phys. **11**, 013023 (2009).
[13] E. M. Hankiewicz and G. Vignale, J. Phys.: Condens. Matter **21**, 253202 (2009).
[14] G. Vignale, J. Supercond. Nov. Magn. **23**, 3 (2010).
[15] M. I. Dyakonov and V. I. Perel, Phys. Lett. A **35**, 459 (1971).
[16] A. G. Aronov and Yu. B. Lyanda-Geller, JETP Lett. **50**, 431 (1989).
[17] V. Edelstein, Solid State Commun. **73**, 233 (1990).
[18] Y. K. Kato, R. C. Myers, A. C. Gossard, and D. D. Awschalom, Science **306**, 1910 (2004).
[19] V. Sih, R. C. Myers, Y. K. Kato, W. H. Lau, A. C. Gossard, and D. D. Awschalom, Nat. Phys. **1**, 31 (2005).
[20] J. Wunderlich, B. Kaestner, J. Sinova, and T. Jungwirth, Phys. Rev. Lett. **94**, 047204 (2005).
[21] N. P. Stern, S. Ghosh, G. Xiang, M. Zhu, N. Samarth, and D. D. Awschalom, Phys. Rev. Lett. **97**, 126603 (2006).
[22] N. P. Stern, D. W. Steuerman, S. Mack, A. C. Gossard, and D. D. Awschalom, Nat. Phys. **4**, 843 (2008).
[23] S. Valenzuela and M. Tinkham, Nature (London) **442**, 176 (2006).
[24] T. Kimura, Y. Otani, T. Sato, S. Takahashi, and S. Maekawa, Phys. Rev. Lett. **98**, 156601 (2007).
[25] T. Seki, Y. Hasegawa, S. Mitani, S. Takahashi, H. Imamura, S. Maekawa, J. Nitta, and K. Takanashi, Nat. Mater. **7**, 125 (2008).
[26] I. Mihai Miron, G. Gaudin, S. Auffret, B. Rodmacq, A. Schuhl, S. Pizzini, J. Vogel, and P. Gambardella, Nat. Mater. **9**, 230 (2010).
[27] J.-i. Inoue, G. E. W. Bauer, and L. W. Molenkamp, Phys. Rev. B **67**, 033104 (2003).
[28] C. L. Yang, H. T. He, L. Ding, L. J. Cui, Y. P. Zeng, J. N. Wang, and W. K. Ge, Phys. Rev. Lett. **96**, 186605 (2006).
[29] H. J. Chang, T. W. Chen, J. W. Chen, W. C. Hong, W. C. Tsai, Y. F. Chen, and G. Y. Guo, Phys. Rev. Lett. **98**, 136403 (2007).
[30] W. F. Koehl, M. H. Wong, C. Poblenz, B. Swenson, U. K. Mishra, J. S. Speck, and D. D. Awschalom, Appl. Phys. Lett. **95**, 072110 (2009).
[31] S. Kuhlen, K. Schmalbuch, M. Hagedorn, P. Schlammes, M. Patt, M. Lepsa, G. Güntherodt, and B. Beschoten, Phys. Rev. Lett. **109**, 146603 (2012).
[32] C. Gorini, P. Schwab, M. Dzierzawa, and R. Raimondi, Phys. Rev. B **78**, 125327 (2008).
[33] R. Raimondi and P. Schwab, Europhys. Lett. **87**, 37008 (2009).
[34] K. Shen, G. Vignale, and R. Raimondi, Phys. Rev. Lett **112**, 096601 (2014).
[35] Y. A. Bychkov and E. I. Rashba, J. Phys. C: Solid State Phys. **17**, 6039 (1984).
[36] E. G. Mishchenko, A. V. Shytov, and B. I. Halperin, Phys. Rev. Lett. **93**, 226602 (2004).
[37] R. Raimondi and P. Schwab, Phys. Rev. B **71**, 033311 (2005).
[38] A. Khaetskii, Phys. Rev. Lett. **96**, 056602 (2006).
[39] V. K. Dugaev, M. Inglot, E. Y. Sherman, and J. Barnaś, Phys. Rev. B **82**, 121310 (2010).
[40] L. X. Hayden, R. Raimondi, M. E. Flatté, and G. Vignale, Phys. Rev. B **88**, 075405 (2013).
[41] X. Wang, J. Xiao, A. Manchon, and S. Maekawa, Phys. Rev. B **87**, 081407 (2013).

[42] S. D. Ganichev, E. L. Ivchenko, V. V. Bel'kov, S. A. Tarasenko, M. Sollinger, D. Weiss, W. Wegscheider, and W. Prettl, Nature (London) **417**, 153 (2002).
[43] I. V. Tokatly, Phys. Rev. Lett. **101**, 106601 (2008).
[44] C. Gorini, P. Schwab, R. Raimondi, and A. L. Shelankov, Phys. Rev. B **82**, 195316 (2010).
[45] A. Takeuchi and N. Nagaosa, arXiv:1309.4205.
[46] R. Raimondi, P. Schwab, C. Gorini, and G. Vignale, Ann. Phys. (Berlin) **524**, 153 (2012).
[47] A. G. Rybkin, A. M. Shikin, V. K. Adamchuk, D. Marchenko, C. Biswas, A. Varykhalov, and O. Rader, Phys. Rev. B **82**, 233403 (2010).
[48] S. Mathias, A. Ruffing, F. Deicke, M. Wiesenmayer, I. Sakar, G. Bihlmayer, E. V. Chulkov, Y. M. Koroteev, P. M. Echenique, M. Bauer, and M. Aeschlimann, Phys. Rev. Lett. **104**, 066802 (2010).
[49] H. A. Engel, B. I. Halperin, and E. I. Rashba, Phys. Rev. Lett. **95**, 166605 (2005).
[50] J. C. R. Sánchez, L. Vila, G. Desfonds, S. Gambarelli, J. P. Attané, J. M. D. Teresa, C. Magén, and A. Fert, Nat. Commun. **4**, 2944 (2013).
[51] Y. Niimi, Y. Kawanishi, D. H. Wei, C. Deranlot, H. X. Yang, M. Chshiev, T. Valet, A. Fert, and Y. Otani, Phys. Rev. Lett. **109**, 156602 (2012).
[52] R. Winkler, *Spin-orbit Coupling Effects in Two-dimensional Electron and Hole Systems* (Springer, Berlin, 2003).